Polymer Bulletin 49, 173-180 (2002)

Polymer Bulletin

Control of the photorefractive effect using a low T_g sol-gel glass

Dong Hoon Choi (✉) , Woongi Jun, Kwang Yong Oh, Jae Hong Kim

College of Environment and Applied Chemistry, Materials Center for Information Display, Institute of Natural Sciences, Kyung Hee University, Yongin, Kyungki 449-701 Korea
E-mail: dhchoi@khu.ac.kr

Received:27 May 2002/Revised version:23 August 2002/Accepted:7 September 2002

Summary

We prepared the photorefractive sol-gel glass based on organic-inorganic hybrid materials containing a charge transporting molecule, second-order nonlinear optical chromophore, photosensitizer, and plasticizer. Carbazole and 2-{4-[(2-hydroxyethyl) methylamino]benzylidene}malononitrile were reacted with 3-isocyanatopropyl triethoxysilane and the functionalized silanes were employed to fabricate the efficient photorefractive media including 2,4,7-trinitrofluorenone (TNF) to form a charge transfer complex. The simplest way to vary the composition in the matrix was to mix the desired amount of the functionalized alkoxysilane. The prepared sol-gel glass samples contained a large amount of nonlinear optical (NLO) chromophore compared to that of the charge transporting molecules. They showed a large net gain coefficient and high diffraction efficiency at certain conditions.

Introduction

Photorefractive (PR) materials have much attention as principal candidates for the medium of real time holographic display.[1-4] Organic PR materials are considered to be the most promising ones since they possess unique advantages such as the highest figure of merit, structural flexibility, ease of fabrication, low dielectric constant, and low cost compared to inorganic PR crystalline materials. [5-10]

The photorefractive effect can be observed in a bifunctional organic material system that exhibits photoconductivity and electro-optic properties. The charge carriers generated in the bright regions of a spatially modulated light migrate by thermal diffusion or under an applied electric field and become trapped in the dark regions, resulting in the formation of a nonuniform space charge field. The modulation of the refractive index is caused, *via* Pockels effect, by the induced internal electric field.

Among many kinds of fabrication method for photorefractive samples, organic and inorganic hybrid materials prepared through sol-gel process have been attractive due to simple and easy method. [11-13] Compared to organic polymers, it can be prepared by simple hydrolysis and condensation process at low temperature using the functionalized silanes and many kinds of guest molecules. Silicon trialkoxide derivatives can be simply designed to bear a functional group in one arm of silicon

through a flexible spacer. The resultant chemical structure of the sol-gel material used herein is quite similar to that of the functional side-chain copolymers. The synthesis of the functionalized silane is also very easy and it can give us a well-defined bulk matrix containing the desired amount of the functional molecules.
In this work, we fabricated the sol-gel glass samples varying the concentration of each component for showing the photorefractive effect and reported a high net gain and high diffraction efficiency. The specific plasticizer was selected, which is well miscible with the matrix molecules. The designed sol-gel glass was considered to show photoconductivity due to carbazole moiety and also electro-optic property due to the push-pull nonlinear optical (NLO) active chromophore.

Experimental

The structures of the functional compounds that were employed to prepare the PR composite were illustrated in Figure 1. SG-Cz is the silane bearing a carbazole unit and SG-MN acts as a second-order nonlinear optical chromophore. For preparing the viscous solution to fabricate the thick film, SG-Cz and SG-MN were dissolved in tetrahydrofuran(THF). Water and hydrochloric acid were added into the solution for hydrolysis and condensation. The molar composition of the solution is as follows: SG-Cz/SG-MN: H_2O: HCl: THF= 1: 4: 0.02: 4. The viscous solution was stirred at room temperature for 6 hours. The solution was filtered through acrodisc syringe filter (Millipore 0.2 μm) and then cast on the indium tin oxide (ITO) pre-coated glass. The film was dried overnight at 80°C under vacuum. After the solvent was removed completely, another ITO glass was placed on the top of the film and then pressed down at 80°C using the 75 μm polyimide film as a spacer to get a sandwich sample for the two-beam coupling (2BC) and the degenerated four wave mixing (DFWM) experiments.

Instruments: UV-Vis absorption spectroscopy was performed on a Hewlett Packard 8453 spectrophotometer (PDA type, λ=190-1100 nm). The thermal property of the sol-gel sample was investigated by differential scanning calorimetry (DSC) using a Perkin Erlmer DSC7. The heating rate was 10°C/min in all cases.

Measurement of the electric field induced birefringence: The electro-optic property of the sol-gel glasses was studied by using the transmission ellipsometric method. The sample tilted by 45° was mounted between the crossed polarizers (±45°). The electric field induced birefringence (Δn) of the sol-gel glass was monitored by virtue of the transmitted beam intensity (T) through crossed polarizers under an applied electric field, as described by the following equation (1).

$$T = \sin^2 (2\pi/\lambda \cdot l \cdot \Delta n) \text{ -----(1)}$$

where λ is the wavelength and l is a distance of light path.

Photorefractivity: Photorefractivity measurements were conducted with a two-beam coupling technique (2BC) and a degenerated four wave mixing (DFWM) technique at 23°C. In a two-beam coupling experiment, A 633 nm wavelength He-Ne laser was incident on the sample and two p-polarized laser beams with an equal intensity of

60.7mW/cm^2 were coupled on the sample to write the refractive index grating. The incident-crossing angle of the beams is 6°, and the film normal was tilted at an angle of 50° with respect to the symmetric axis of the two writing beams. The transmitted intensities of both beams were detected using two calibrated photodetectors (Newport, Model 1815-C, Photodiode, 818-SL) and were recorded with a personal computer.
For the degenerated four-wave mixing experiment, two s-polarized beams (I=70mW/cm^2) were used as writing beams and a p-polarized reading beam with the intensity of 1mW/cm^2 counterpropagated to one of the writing beams. The normal of the sample surface was tilted 50° with respect to the symmetric axis of the two intersected beams, and the angle between the two-coupled beams was set to be 20°. In the DFWM experiment, the diffraction efficiency was determined by the ratio of the intensity of the diffracted signal to that of the incident reading beam and the dynamic behavior was also observed.

Results and discussion

First, we prepared the second-order NLO active and charge transporting triethoxysilanes (SG-MN & SG-Cz) by simple reaction between alcohol and isocyanate group. SG-MN and SG-Cz are well soluble in THF, dichloromethane, acetone, dimethylformamide, pyridine etc. The structures of the functional silicon alkoxide compounds that were employed to prepare the PR sample were illustrated in Figure 1 including photosensitizer and plasticizer used in this study. Polyethylene glycol (M_n~ 600) was employed as a plasticiser in this sol-gel matrix. The hydrogen bond between the hydroxyl and ether group in polyethylene glycol and secondary amine of urethane group in the side chain of the alkoxysilane improved the miscibility preventing from phase separation.[14] TNF was also used as a photocharge generating sensitizer to be doped into the sample. In Table I, the compositions of three prepared samples were described.

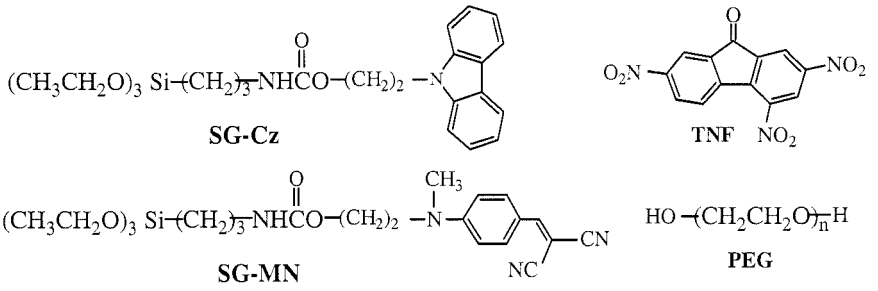

Figure 1. Chemical structures of the compounds used in the photorefractive sol-gel glass.

The thermal behavior of the sol-gel composite sample was investigated by differential scanning calorimetry (DSC). Most of the low T_g PR polymer showed glassy-rubbery transition around 20-30°C, however, in this sol-gel glass those values descended to 2-16°C to enhance the molecular orientational ability during poling. (See Figure 2) This indicates that we can manipulate the physical properties just by changing the concentration of each component. There is one thing that should be emphasized in this

study. We can control the photoconductivity and electro-optic properties by simply changing the composition of additive components, which is advantageous for exhibiting the PR properties over guest-host system and organic multifunctional

Table 1. Composition and properties of three different sol-gel PR samples.

	Composition(wt%)				T_g(°C)	α(cm^{-1}) at 633nm	S (10^{-12}x $cm(\Omega W)^{-1}$)	η(%) [E_p=80V/μm]
	SG-Cz	SG-MN	TNF	PEG				
Sample I	30.1	60.2	0.7	9.0	7	65.9	7.0	56
Sample II	45.0	45.0	1.0	9.0	2	62.7	10.3	44
Sample III	59.8	29.9	1.3	9.0	16	57.4	20.6	2.0

*T_g was determined by measuring the 1st onset temperature in 2nd heating cycle.
*S: Photoconductivity Sensitivity

copolymers. Therefore, the exact desired composition can be elaborated for varying the PR properties.

The sample II showed the lowest T_g around 2°C among three samples although the thermal history is identical during preparing the PR sample. The sample I and III showed T_g around 7 °C and 16 °C, respectively. For this reason, the second-order NLO chromophores can be easily reoriented by applying a dc electric field in all samples at room temperature. Therefore, all three samples were not poled prior to PR

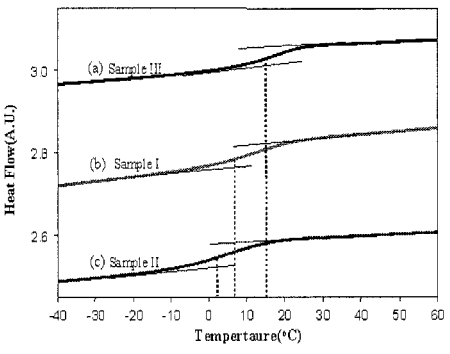

Figure 2. DSC thermograms of three different sol-gel PR samples.

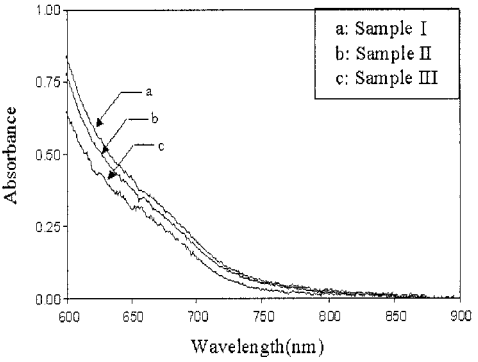

Figure 3. UV-Vis absorption spectra sol-gel PR samples.

measurement. In Figure 3, we investigated the absorption property of the PR samples with three different compositions of SG-Cz and SG-MN. All samples showed broad absorption band around 650-700 nm. The difference of the absorbance value in that range is attributed to the concentration of the NLO chromophore mainly. Their absorption coefficients of three samples at 633 nm are shown in Table 1. Absorption coefficient, α is related to the concentration of the NLO chromophore and TNF in the charge transfer complex proportionally. Therefore, the sample I showed the highest absorption coefficient at 633 nm.

Electric field induced optical anisotropy of the PR sample was studied by way of the transmission technique. Using the transmission value under crossed polarizers, we

could calculate the birefringence value and plot the relation between the birefringence and the applied electric field. As shown in Figure 4, the birefringence increased with the applied electric field, which is strongly ascribed to the degree of orientation of NLO chromophore in the sol-gel glass. Sample I showed higher birefringence compared to those of sample II and III over a whole range of the applied electric field. It is well recognized that the birefringence is strongly dependent on the concentration of NLO chromophore.

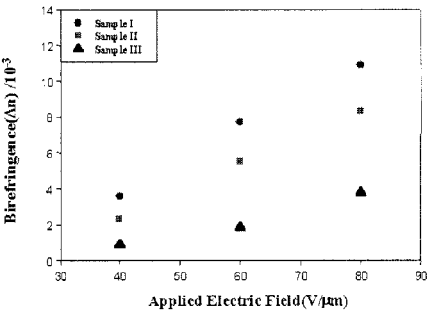

Figure 4. Birefringence of three sol-gel samples under an electric field.

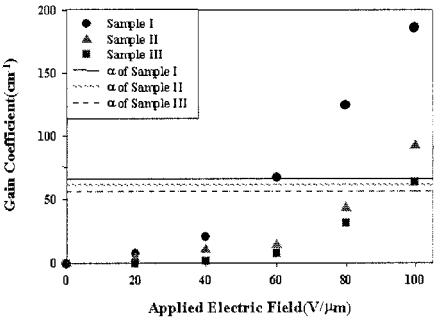

Figure 5. Coupling coefficients as a function of the applied electric field.

Photorefractivity measurements were conducted with a two-beam coupling (2BC) and a degenerated four wave mixing (DFWM) technique after applying d.c. voltage for 10 min. for saturated molecular orientation. A 633 nm wavelength He-Ne laser was incident on the sample. Resulting from the two-beam coupling experiment, optical coupling gain coefficient (Γ) was calculated according to the equation (2).

$$\Gamma = (1/L) \times \ln [\gamma / (2-\gamma)] \text{--------(2)}$$

where L is the optical path for the amplified beam and γ is the beam coupling ratio (the ratio of the signal intensities with and without pump beam). The calculated gain coefficients due to the energy transfer between the two beams are shown in Figure 5. The sample I comprised much higher concentration of the NLO chromophore. It showed higher optical coupling gain coefficient over whole range of the applied electric field. The maximum net gain was observed to be higher than 125 cm^{-1} although the absorption coefficient is measured to be 65.9 cm^{-1}. The photoconductivity sensitivity measured under an applied electric field of 100V/μm was shown in Table 1. As we expected, although the photoconductivity was found higher in the sample III due to a higher concentration of photocharge generating and charge transporting molecule (SG-Cz), the gain was observed relatively lower resulting from the lower concentration of the NLO chromophore. There should be a balance of concentration between the charge transporting molecules and NLO chromophore to exhibit a significant photorefractive effect. In these sol-gel glasses, the effect of the concentration of the NLO chromophore and the birefringence was also found pronounced accompanying with the effect of the charge transporting molecules.

Under the fixed molar concentration of SG-Cz and TNF, only thing we can consider is

the effect of the induced birefringence value and the concentration of the NLO chromophore to change the performance of PR matrix. The glass transition temperature of the sample I is 7°C higher than that of the sample II. However, the density of the NLO chromophore contributes to raise the PR effect predominantly. There are few reports on the PR properties of the samples containing much higher NLO chromophore than that of charge transporting molecules because of difficulties in synthesis and phase separation in guest-host system. In this sol-gel process, we can fully optimize the composition to show significantly high performance in photorefractivity.

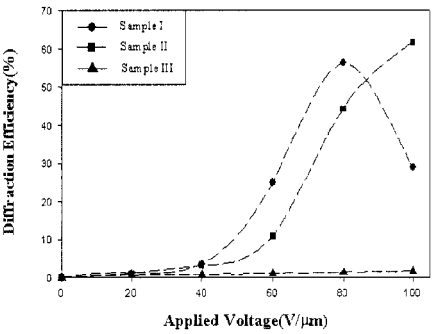

Figure 6. diffraction efficiency as a function of the applied electric field.

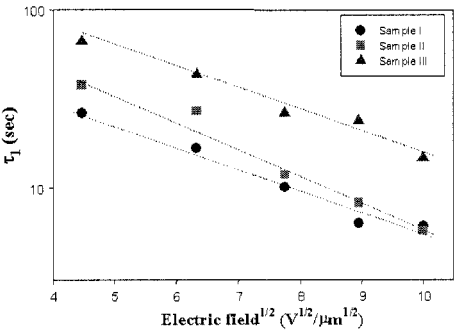

Figure 7. Fast response time as a function of the applied electric field.

In the DFWM experiment, the diffraction efficiency (η) was determined by the ratio of the intensity of the diffracted signal to that of the incident reading beam. We also observed the growing and decaying behavior of the diffraction efficiency. Figure 6 shows the electric field dependence of the diffraction efficiency. The diffraction efficiency increased with the applied electric field and the maximum diffraction efficiency of sample I was achieved at 80V/μm. That is attributed to the highest concentration of the NLO chromophore and the high birefringence. Although the field dependence of the steady-state diffraction efficiency of the sample I was well described by the Kogelnik coupled-wave model, the η value was determined relatively lower than we expected.[15] Reflectivity loss at the material interfaces was observed in sample I at a high electric field (>60V/μm). This is why the η value of sample II at 100V/μm is higher than that of the maximum η value of the sample I.

The dynamics of the holographic grating formation were studied by measuring the time constants of the grating formation in the DFWM experiment. Quantitative information about the grating growth can be obtained by an empirical double exponential function of the following equation (3) fitted to the data of diffraction efficiency.

$$\eta(t) = \eta_o [\ 1-(a \exp(-t/\tau_1)+(1-a) \exp(-t/\tau_2))]^2 \text{---(3)}$$

where a, τ_1, and τ_2 are the three fitting parameters. η_o is the steady state diffraction efficiency. The fast rate constant of the diffraction efficiency is indicated by the first term of the equation. Such a fast response time may be attributed to large charge carrier mobility and facile NLO chromophore orientation in the sol-gel matrix. In

Figure 7, we describe the dependence of the fast rate constants describing the rising of the space charge field and the molecular orderness of the second-order NLO chromophore. Sample III showed very slow grating formation in the range of 14.7-66.7 sec. On the other hand the fast time constants of sample I and II were observed to be 6.1-26.3 and 5.7-37.7 sec, respectively. It is considered by the fast rate constants that the concentration of the NLO chromophore and the rigidity of the matrix affect the dynamics of PR grating formation with the charge carrier generation and its mobility, and the hole trap density.

The potential of PR sol-gel sample (e.g. Sample I) was evaluated for a holographic recording using 75 μm thick sandwich sample. Figure 8 (A) is the original target image through the sol-gel glass sample. The image was recorded at the external applied field of 80V/μm and the stored image is reconstructed by illuminating of the probe beam. In Figure 8(B), the reconstructed hologram image was illustrated and the image can be erased by irradiation of the reference beam blocking the objective beam. This results in the possibility of the sol-gel sample applicable to the holographic recording medium although contrast and resolution should be improved furthermore.

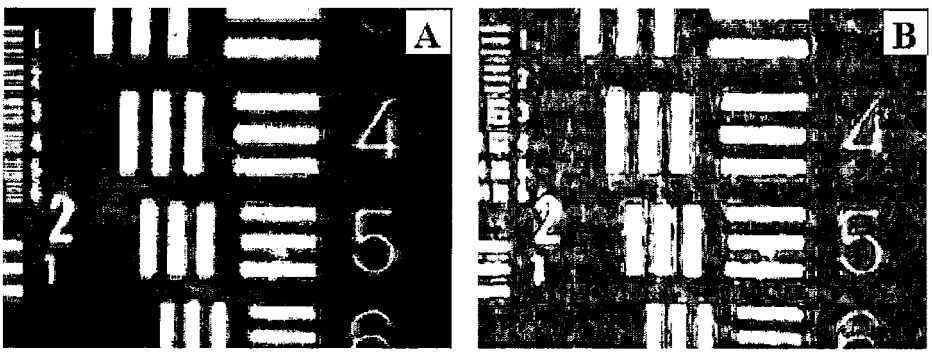

Figure 8. Photographs of (A) original image transmitted through the sample I and (B) the reconstructed hologram image.

CONCLUSION

The photorefractive properties of a new series of sol-gel composite materials have been presented. Charge photogeneration is facilitated by doping a sensitizer, TNF. Two miscible molecules such as SG-Cz and SG-MN provide the charge transporting and the second order NLO properties. PEG behaves as a well miscible plasticizer due to hydrogen bond formation. Resulting from the 2BC and DFWM experiment, sample I showed best performance of PR property. Resulting from the dynamic behavior of the diffraction efficiency, the fast response time, τ_1 was found to be affected by the rate of formation of the space charge field and the glass transition temperature of the sol-gel PR sample. Also, we stored the holographic information successfully using the sol-gel PR sample (e.g. Sample I).

Acknowledgement. This research was supported by the Korea Science and Engineering Foundation (contract # R01-2000-00338-0).

References

1. Volodin BL, Sandalphon R, Meerholz K, Kippelen B, Kukhtarev NV, Peyghaambarian N (1995) Opt Eng 34: 2213.
2. Chang CJ, Whang WT, Hsu CC, Ding ZY, Hsu KY, Lin SH (1999) Macromolecules 32: 5637.
3. Strutz SJ, Hayden LM (1999) Appl Phys Lett 74: 2749.
4. Goonesekera A, Wright D, Moerner WE (2000) Appl Phys Lett 76: 3358.
5. Steenwinckel DV, Engels C, Gubbelmans E, Hendrickx E, Samyn C, Persoons A (2000) Macromolecules 33: 4074.
6. Moon H, Hwang J, Kim N, Park SY (2000) Macromolecules 33:5116.
7. Okamoto K, Nomura T, Park SH, Ogino K, Sato H (1999) Chem Mater 11: 3279 .
8. Ho MS, Barrett C, Paterson J, Esteghamatian M, Natansohn A, Rochon P (1996) Macromolecules 29: 4613.
9. Peng Z, Gharavi AR, Yu L (1997) J Am Chem Soc 119: 4622.
10. Sohn J, Hwang J, Park SY, Lee JK, Lee JH, Chang JS, Lee GJ, Zhang B, Gong Q (2000) Appl Phys Lett 77: 1422.
11. Darracq B, Chaput F, Lahlil K, Boilot JP, Levy Y, Alain V, Ventelon L, Desce MB (1998) Optical Mater 9: 265.
12. Hsiue GH, Kuo WJ, Lin CH, Jeng RJ, Macromol Chem Phys 17: 2336.
13. Darracq B, Canva M, Chaput F, Boilot JP, Riehl D, Levy Y, Brun A (1997) Appl Phys Lett 70: 292.
14. Choi DH, Oh KY, Jun WG (2002) Opt Mater in press.
15. Kogelnik H (1969) Bell Syst Tech J 48: 2909.